Contents

6. Numerical Simulation of Spacecraft Charging Phenomena

J.G. Laframboise and S.M.L. Prokopenko
Physics Department
York University
Toronto, Canada

Abstract

A numerical simulation program is being constructed having the following features: (1) infinite circular cylindrical geometry with angle-dependence, (2) inclusion of incident particles, photoelectrons, secondary electrons, backscattered electrons, any gun emissions, and any internal current pathways including surface conductive layers, (3) "quasistatic time-dependent iteration", in which sheath potential changes during particle transit times are ignored, (4) use of approximate, locally-dependent space charge density expressions in solving Poisson's equation for sheath potentials, with use of numerical orbit-following to determine surface currents, (5) incident particle velocity distributions isotropic or beam-like, or some superposition of these. Rationales for each of these features are discussed.

1. INTRODUCTION

The asymmetry between sunlit and shaded areas of a synchronous spacecraft is a key feature of the differential spacecraft charging problem at synchronous altitude. A realistic numerical model for the plasma sheath surrounding a

synchronous spacecraft must therefore be at least two-dimensional. The only existing two-dimensional simulation which is completely self-consistent is that of Soop,[1] who did a time-dependent treatment for a sphere, in which several thousand photoelectrons were followed numerically. Such time-dependent treatments have until now provided relatively low accuracy for a given computational expense, although there now exist improved interpolation techniques for deducing space charge and flux from a limited amount of orbit information, which may change this situation in the future.

Two other more simplified treatments are noteworthy. Schröder[2] assumed that photoelectron emission was spherically symmetric, and thereby obtained a self-consistent solution for a unipotential sphere, which showed the presence of potential minima due to photoelectron space charge in some circumstances. Lafon[3] assumed spherical or cylindrical symmetry for space charge due to ambient particles, and negligible perturbation of this symmetry by photoelectrons. He thus obtained radially symmetric self-consistent sheath potentials, but angle-dependent photoelectron density profiles, again for unipotential spheres and cylinders.

Here we describe a two-dimensional self-consistent simulation which avoids a completely time-dependent treatment, but instead is based on a "quasistatic time-dependent" iteration described in Section 2.2. Although results from three-dimensional simulations are likely to become available in the near future,[4] it is generally true that the simplest realistic simulations are advantageous in elucidating basic physical effects, whereas more complicated ones are most useful for quantitatively predicting detailed interactions.

2. FEATURES OF NUMERICAL SPACECRAFT – CHARGING MODEL

2.1 Infinite Circular Cylindrical Geometry with Angle-Dependence

This geometry implies the use of a polar coordinate grid for computations. Several reasons for such a choice, in preference to the more obvious spherical geometry, are:

(1) Although a spherical geometry, with rotational (azimuthal) symmetry about the spacecraft-sun axis, is two-dimensional in position space, it is three-dimensional in velocity space because particles with different azimuthal angular momenta must be treated separately.

(2) Many spacecraft are finite circular cylinders.

(3) In spherical geometry with azimuthal symmetry, focusing of particles onto the spacecraft-sun axis occurs in some models, leading to singularities in fluxes and densities along this axis. Such effects must be regarded as spurious since real spacecraft are unlikely to have the high degree of symmetry necessary to produce them.

(4) An infinite cylinder, having a surface sector with distinct properties, can be rotated with respect to the sunward direction to study the effects of such rotation. In a spherical geometry with azimuthal symmetry, the corresponding surface feature would be an annulus about the spacecraft-sun axis, and no such rotation would be possible without destroying azimuthal symmetry.

(5) One major feature of spherical as opposed to cylindrical geometry, that is, the more rapid decrease of potential with increasing radius, can be modeled in an approximate way by simply adding the appropriate fictitious contribution to $\nabla^2\phi$ in Poisson's equation.

2.2 Physical Processes

The model is to include velocity distributions of: incident particles, photoelectrons, secondary electrons, backscattered electrons, and any gun emissions. Internal current pathways including surface conductive layers are also being included.

2.3 Quasistatic Time-Dependent Iteration

In this procedure, sheath potential changes during particle transit times are ignored. This leads to the following iteration scheme: An angle-dependent surface potential is chosen. Poisson's equation is then solved to provide a radius- and angle-dependent static sheath potential (see Section 2.4 below). Particle orbits are then followed numerically in this potential, yielding surface charging rate as a function of angle (orbit-following is, however, not used to provide space charge densities for Poisson's equation; see Section 2.4 below). These rates are then averaged over any conducting sector, and any currents transferred internally (including those through any surface conductive layers) are subtracted. The resulting net charging rates are then used to carry forward one time step, yielding new surface potentials. This process is then repeated until a steady-state condition results, or, in a situation in which external conditions vary with time, is repeated to follow such time-dependence.

The use of this procedure, as opposed to a completely time-dependent simulation, should produce important computational economies. Clearly one will lose information about very rapid transient phenomena with this approach. However, steady-state or slowly time-varying situations are of major importance. These include changes in the incident particle distributions, which are likely to have time scales of seconds or minutes.

2.4 Use of Approximate Space-Charge Density Expressions

At synchronous altitude, the Debye length λ_D for ambient particles is usually $\gtrsim 10$ m, so for satellites of ordinary size, effects of ambient space charge on sheath potentials will be relatively small. Any reasonably realistic approximation of this space charge can therefore be expected to produce only negligible errors in solving Poisson's equation for sheath potentials. Furthermore, large savings in computer time can be expected to result if one can avoid exact density calculations involving numerical orbit-following. In the present work, it is intended that a relatively small amount of orbit-following be done to calculate surface currents (Section 2.3).

A more significant space-charge effect near the spacecraft may be caused by emitted photoelectrons or secondary electrons,[1,2] because of their relatively low velocities compared to ambient values. However, effects of these are likely to also be small enough that any reasonably realistic approximations for their densities will yield good accuracy.[3] Such approximations must ultimately be validated by comparison with a few carefully chosen exact calculations. It is advantageous if such approximations depend on local potential only (rather than potentials at many locations), together with a relatively small number of other parameters, such as spacecraft potentials and potential barrier heights and locations. Here we propose three types of space-charge density approximation, as follows.

2.4.1 APPROXIMATIONS FOR POTENTIAL WELLS WITHOUT OBSTACLES

Exact density expressions have been developed for collisionless, Maxwellian particles in the presence of obstacle-free potential wells of arbitrary shape by Laframboise and Parker.[5] The appropriate expression for our purposes is the result given by their Eq. (2) for three-dimensional wells. This is true even for an "infinite", that is, very long cylindrical spacecraft geometry, because of particle entry at the ends of such a geometry. For definiteness, we consider a negative well given by $\phi(x, y, z) \leq 0$, with $\phi \to 0$ as $x^2 + y^2 + z^2 \to \infty$, where ϕ is electric potential. If only ambient particles are considered, Poisson's equation is:

$$\nabla^2 \phi = \frac{e}{\varepsilon_o} (N_e - N_i) \tag{1}$$

where e is magnitude of unit electron charge, ε_o is permittivity of space, and N_e, N_i are electron and ion number densities, respectively. Since positive ions are the attracted species in this well, we use Eq. (2) of Laframboise and Parker[5] for ion density, and the usual Boltzmann factor for electron density. If $\lambda_{De} = (\varepsilon_o kT_e / e^2 N_\infty)^{1/2}$, N_∞ is electron or ion density far from the spacecraft,

L is a characteristic spacecraft length, $\tilde{\nabla} = L\nabla$, $\chi = e\phi/kT_e < 0$, k is Boltzmann's constant and T is temperature, Eq. (1) becomes:

$$\tilde{\nabla}^2 \chi = \left(\frac{L}{\lambda_{De}}\right)^2 \left\{ e^{\chi} - \frac{2}{\sqrt{\pi}} \left[(-\chi\, T_e/T_i)^{1/2} + g\ (-\chi\, T_e/T_i)^{1/2} \right] \right\} \tag{2}$$

where $g(s) = \frac{1}{2}\sqrt{\pi}\, \exp(s^2)\mathrm{erfc}(s) = \exp(s^2) \int_s^\infty \exp(-t^2)dt$.

The important feature of Eq. (2) for our purposes is that its right-hand side is a function of χ only. For small χ, Eq. (2) reduces to:

$$\tilde{\nabla}^2 \chi = (1 + T_e/T_i)(L/\lambda_{De})^2\, \chi \tag{3}$$

where terms of order $\chi^{3/2}$ and higher have been ignored. The linear form of (3) permits the use of direct Poisson-solvers for finding χ. Another simplified form can be obtained by rederiving Eq. (2) with monoenergetic instead of Maxwellian ions assumed. The appropriate monoenergetic velocity distribution (Chen;[6] Laframboise,[7] p. 14) is:

$$f \equiv \frac{d^3N}{d^3\underline{v}} = \frac{m_i^2 N_\infty}{4\pi} \frac{\delta(E - E_1)}{(2m_i E_1)^{1/2}} \tag{4}$$

where $E_1 = 4kT_i/\pi$ and m_i is ion mass; this distribution duplicates the ambient number density and flux values of a Maxwellian at temperature T_i. Rederivation of (2) using this distribution yields the computationally simpler form:

$$\tilde{\nabla}^2 \chi = \left(\frac{L}{\lambda_{De}}\right)^2 \left[e^{\chi} - \left(1 - \frac{\pi}{4}\frac{T_e}{T_i}\chi\right)^{1/2} \right] . \tag{5}$$

If any regions exist where $\chi > 0$, the roles of ions and electrons are interchanged, and Eqs. (2)-(5) must be modified accordingly.

The essential approximation contained in Eqs. (2) - (5) is the neglect of orbit depletion due to intersection with the spacecraft. The densities of ambient ions and electrons will therefore both be overestimated near the spacecraft in these results. As long as the spacecraft is at least moderately smaller than λ_{De}, the effects of this overestimate will be small. The attracted-species density will be overestimated by the greater amount for reasons involving the curvatures of attracted and repelled particle orbits. The sheath profiles predicted by (2) or (5) will therefore be steeper than real profiles, if electron emission effects are ignored.

2.4.2 APPROXIMATIONS BASED ON SYMMETRIC POTENTIALS

Laframboise,[7] and Laframboise and Godard,[8] Eqs. (7) and (8), have presented expressions for number densities of ambient attracted and repelled Maxwellian particles, respectively, which are exact for radially symmetric monotonic potentials near a perfectly absorbing spherical collector. These expressions contain terms identical to the ion and electron density expressions in (2), together with subtractive terms representing the effects of particle interception by the collector. Whipple[9] has used a thick-sheath approximation to develop density expressions for both ambient and emitted particles in the presence of a potential barrier, again for spherical symmetry. Lafon[3] has developed approximate density expressions for escaping photoelectrons, based on assumed spherical or cylindrical symmetry in the sheath potential, but not in the photoemission fluxes. Since all of these expressions depend only on local potential and a small number of other parameters, it is tempting to explore the possibility of using them even in the presence of sheath potentials which are known to be angle-dependent, and near spacecraft having nonspherical shapes. All of these expressions depend essentially on the solid angles subtended at any given radius, by orbits which have intersected the spacecraft, for all significantly populated particle energies, including[7, 8, 9] the effects of orbit curvature due to electric fields. It is likely that in many cases, such solid angles will not be greatly modified by angular asymmetries in sheath potentials (from symmetry, such modification must be of second order in angular variations). In using such approximations with irregular spacecraft shapes, it would be necessary to define some way of choosing "radius" for substitution into them. One way to do this would involve matching the solid angle subtended by the spacecraft at the location in question, with that subtended by a sphere as a function of radius. Similar procedures would be necessary for dealing with parameters describing potential barriers in these expressions. Lafon[10, 11] and Parker[12] have given useful general discussions of the formulation of density expressions for symmetric potentials.

2.4.3 APPROXIMATIONS BASED ON EQUIVALENT POTENTIAL WELLS

We consider the idealized situation shown in Figure 1, in which a spacecraft is assumed to have shaded-side surface potentials which are very negative, and sunlit-side surface potentials which are close to space potential. The solid curves outside the spacecraft represent equipotentials. The dotted curve FGH represents a surface which passes through the saddle point G on the sunlit side, and is everywhere perpendicular to the equipotentials, so this surface represents the maximum extent of a sunlit-side potential barrier for electrons. Fahleson[13] has pointed out that such a barrier may exist even when space charge is negligible, because of the

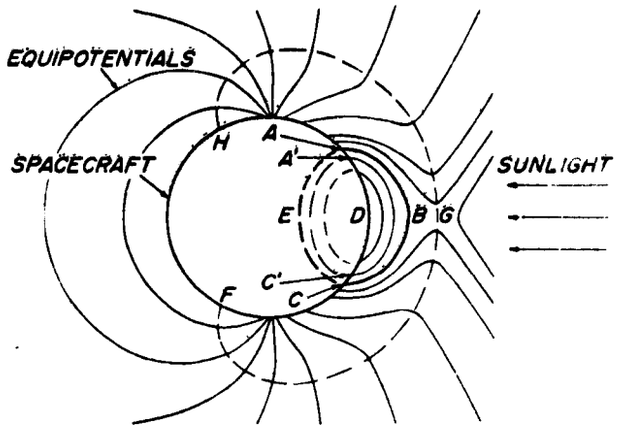

Figure 1. General Appearance of a Possible Sheath Potential Profile around a Spacecraft. Dotted curves inside the spacecraft surface are fictitious extensions of equipotential surfaces outside, as described following Eq. (6)

sunlit-shaded asymmetry in surface potentials. We consider as an example the process of approximately calculating photoelectron space charge density inside this barrier; calculation of secondary electron charge density is similar in most respects. We consider all those photoelectrons emitted with a total energy E_B equal (within some differential amount dE) to the potential of the equipotential surface ABC. Such particles can never go outside ABC, but must reimpinge on the spacecraft surface ADC. If $\xi_p(E)$ is the photoemission coefficient, that is, the energy-differential particle current density of photoemission from the spacecraft surface (this will depend on surface material and solar illumination angle), then the total photoemission particle current between energies E_B and $E_B + dE$ is:

$$I_p = dE \iint d^2 S \, \xi_p \left[E_B + e\phi_S, \; S \right] \tag{6}$$

where $E_B + e\phi_S \geq 0$, S represents surface position, $\phi_S \equiv \phi(\underline{r}_S)$ is surface potential, $E_B + e\phi_A = E_B + e\phi_C = 0$, and the integration is over the surface ADC. Since ξ_p for most materials is largest for emission kinetic energies $\frac{1}{2} m_e v^2 = E_B + e\phi_S \approx 1$ volt, most of the photoemission between energies E_B and $E_B + dE$ will tend to come from regions such as, say, A' and C' in Figure 1, where ϕ_S is about 1 volt more positive than at A and C. On the other hand, particle motions will tend to spread the reimpingement current more uniformly over ADC.

We now model this process approximately by mentally removing the spacecraft surface between A and C, and replacing it by an arbitrary extension AEC of the equipotential surface ABC. We also do the same for other equipotentials which lie inside this one, as also shown in Figure 1. We have now "constructed" an obstacle-free potential well, and we can use the Laframboise-Parker[5] theory to derive model density and flux profiles for such a well. We can then integrate the latter over ADC and match the result with Eq. (6). We rewrite the monoenergetic distribution (4) for electrons as follows:

$$f = \frac{m_e^2 N^*}{4\pi} \frac{\delta(E - E_B)}{(2m_e E_B)^{1/2}} \tag{7}$$

where N^* is now a reference number density to be evaluated. We obtain:

$$N \equiv N[\phi(\underline{r})] = \int f d^3\underline{v} = N^* [1 + e\phi(\underline{r})/E_B]^{1/2} H[e\phi(\underline{r}) + E_B] \tag{8}$$

$$J \equiv J[\phi(\underline{r})] = \int f v_\perp d^3\underline{v} = N^* (E_B/8m_e)^{1/2} [1 + e\phi(\underline{r})/E_B] H[e\phi(\underline{r}) + E_B] \tag{9}$$

where J is a number flux crossing an arbitrarily oriented surface element from either direction, $v_\perp$ is velocity component perpendicular to such a surface element, and $H(s) = \int_{-\infty}^{s} \delta(x)\, dx$ is the Heaviside step function. The total number flux crossing ADC from either direction is now given for our model well by:

$$I_w = \iint J(\phi_S)\, d^2S \quad . \tag{10}$$

Our procedure for approximating the space charge density now involves performing the integrations over the surface ADC in both (6) and (10), then evaluating N^* by equating these two results. This is done for each of the discrete energies E_{Bj} which are chosen to represent the photoemission. The quantity dE in (6) must then be chosen equal to the separation between these energies. The resulting set of values N_j^* is then used together with (8) to construct the space-charge density expression:

$$N[\phi(\underline{r})] = \sum_j N_j^* [1 + e\phi(\underline{r})/E_{Bj}]^{1/2} H[e\phi(\underline{r}) + E_{Bj}] \quad . \tag{11}$$

This expression also has the advantage of dependence only on local potential, as do those derived in Sections 2.4.1 and 2.4.2. In using it, one would precalculate the coefficients N_j^* as described above, then use (11) as a contribution to

the space charge density in Poisson's equation. An important approximation contained in (11) involves neglect of the fact that photoemission fluxes given by (10) are in general distributed differently over ADC than those given by (6). For energies $E_j > -e\phi_G > 0$, where ϕ_G is the saddle-point potential in Figure 1, some photoelectrons would escape, and the corresponding terms in (11) would be overestimates.

2.5 Use of Isotropic or Beam-Like Incident Velocity Distributions

Important computational economies clearly result from assuming that incident velocity distributions are either isotropic or beam-like (monokinetic); the approximate density expressions described in Section 2.4 are examples of results for isotropic distributions. Any incident distribution may be modeled as closely as desired by a superposition of isotropic and beam-like distributions.

3. CONCLUSIONS

We have described the major features of a "quasistatic time-dependent" numerical simulation of differential spacecraft charging at synchronous altitude, incorporating an infinite cylindrical geometry with angle-dependence. The computer program involved is presently under construction.

Acknowledgments

We are indebted to L. W. Parker for valuable discussions. This work was supported by the U. S. Air Force Office of Scientific Research under grant number AFOSR-76-2962.

References

1. Soop, M. (1972) Report on photo-sheath calculation for the satellite GEOS, Planet. Space Sci. 20:859-870.
2. Schröder, H. (1973) Spherically symmetric model of the photoelectron sheath for moderately large plasma Debye lengths. In: Photon and Particle Interactions with Surfaces in Space, R. J. L. Grard, Editor, D. Riedel Pub. Co., Dordrecht, Holland.

3. Lafon, J.-P.J. (1976) On the sheath surrounding a conductor emitting photoelectrons in an isotropic collisionless plasma, Radio Science 11:483-493.

4. Katz, I., Parks, D.E., Wilson, A. (1976) Dynamic modeling of spacecraft in a collisionless plasma, Paper II-7, USAF-NASA Spacecraft Charging Technology Conference, Colorado Springs.

5. Laframboise, J.G., and Parker, L.W. (1973) Probe design for orbit-limited current collection, Phys. Fluids 16:629-636.

6. Chen, F.F. (1965) Numerical computations for ion probe characteristics in a collisionless plasma, Plasma Phys. (J. Nucl. Ener. Part C) 7:47-68.

7. Laframboise, J.G. (1966) Theory of spherical and cylindrical Langmuir probes in a collisionless, Maxwellian plasma at rest, Univ. of Toronto, Institute for Aerospace Studies, Rep. 100.

8. Laframboise, J.G., and Godard, R. (1974) Perturbation of an electrostatic probe by a spacecraft at small speed ratios, Planet. Space Sci. 22:1145-1155.

9. Whipple, E.C., Jr. (1976) Theory of the spherically symmetric photoelectron sheath: a thick sheath approximation and comparison with the ATS 6 observation of a potential barrier, J. Geophys. Res. 81:601-607.

10. Lafon, J.-P.J. (1973) On the perturbation of a plasma and particle collection by a cylinder in a magnetic field, J. Plasma Phys. 10:383-396.

11. Lafon, J.-P.J. (1975) On the behavior of a metallic body in an isotropic collisionless plasma I: General remarks, Plasma Phys. 17:731-740.

12. Parker, L.W. (1975) Computer Method for Satellite Plasma Sheath in Steady-State Spherical Symmetry, AFCRL-TR-75-0410, Final Report, Contract F19628-75-C-0182, Lee W. Parker, Inc.

13. Fahleson, U. (1973) Plasma-vehicle interactions in space: Some aspects of present knowledge and future development, In: Photon and Particle Interactions with Surfaces in Space, R.J.L. Grard, Editor, D. Riedel Pub. Co., Dordrecht, Holland.